Talanta 105 (2013) 15–19

Contents lists available at SciVerse ScienceDirect

Talanta

journal homepage: www.elsevier.com/locate/talanta

Multimethod quantification of Ag^+ release from nanosilver

Madjid Hadioui, Simon Leclerc, Kevin J. Wilkinson *

Department of Chemistry, University of Montreal C.P. 6128, Succursale Centre-Ville Montreal, Canada H3C 3J7

ARTICLE INFO

Article history:
Received 15 August 2012
Received in revised form
21 November 2012
Accepted 22 November 2012
Available online 30 November 2012

Keywords:
Nanosilver
Free metal ion
Nanoparticles
Ion-exchange technique
Single particle ICP-MS
Centrifugal ultrafiltration

ABSTRACT

There is a significant interest in determining the effects of nanomaterials on the environment and human health. Part or all of the toxicity attributed to silver nanoparticles (nAg) may be due to the release of free silver (Ag^+). Therefore, it is necessary to have techniques that will allow the precise determination of free Ag^+ within suspensions of nAg particles. Among the different methods used for the determination of free metals in natural waters, the ion-exchange technique (IET), has promise to both distinguish Ag^+ from nAg and to attain the low detection limits required for the analysis of natural samples. In this paper, IET. centrifugal ultrafiltration and single particle inductively coupled plasma mass spectrometry (SP ICP-MS) were used to determine very low concentrations of free or dissolved Ag in commercial suspensions of nAg. Dilution of the silver nanoparticles played an important role in the measured Ag^+ concentrations. The relative release of Ag^+ from nAg increased as samples were increasingly diluted, implying that it is critical to determine Ag^+ concentrations under the precise conditions used for determinations of toxicological or environmental fate.

1. Introduction

The production and applications of nanomaterials are growing rapidly but their impacts on human health and the environment have not yet been determined unambiguously. Nanosilver (nAg) is among the most common nanomaterials found in consumer products. It is used in a variety of applications including medical, water treatment, cosmetics, clothing and the food industry.

Even though nAg is used for its antimicrobial properties, it is not yet clear whether its toxic effects are due to the release of free silver (Ag^+), nAg or a combination of both species [1–3]. Many studies have identified the potent antimicrobial toxicity of Ag^+ [4] and a few cases of bioavailable Ag complexes [5]. Recently, several research groups have demonstrated the apparent antimicrobial effects of silver nanoparticles [6,7]. For example, in studies using *Escherichia coli*, Kim et al. [6] determined that the antimicrobial activity of nAg was similar to a solution of silver nitrate. Asharani et al. [8] suggested that phenotypical defects in zebrafish were not due to Ag^+ but rather nAg, while both Foldbjerg et al. [9] and Miura and Shinohara [10] reported observing similar biological responses due to nAg and Ag^+. Nonetheless, in most of the studies, nanoparticulates were assumed to predominate in nAg suspensions-free silver was rarely quantified.

Suspensions of nAg contain at least three distinct forms of silver: Ag^0, free Ag^+ (and its soluble complexes) and adsorbed silver [11]. Ions are released from nAg due to oxidation, which can result in the total dissolution of Ag^0 under some conditions. It is difficult to predict the chemical speciation of nAg suspensions, especially in the presence of biological organisms, since equilibrium is not always attained. For example, Navarro et al. [12] suggested that silver particles contributed to toxicity via a Ag^+ release process that was enhanced in the presence of algae due to the production of H_2O_2 (a metabolic product of the algae). Therefore, in order to determine the relative toxicity of Ag^+ with respect to nAg, it is essential to precisely quantify nAg dissolution *under the conditions that are most relevant to the biological or environmental media of interest* (e.g. complex matrices, low nAg concentrations, etc.).

A number of analytical techniques can potentially be used to quantify nAg dissolution in natural and biological media [13]. For example, electrochemical approaches such as anodic stripping voltammetry (ASV), competing ligand exchange with adsorption cathodic stripping voltammetry (CLE-AdCSV) and ion selective electrodes [12,14] have long been used for chemical speciation measurements. Membranes or resins have also been used to separate species on the basis of their charge, size or chemical affinity (e.g. ion exchange technique, IET; Donnan membrane technique, DMT; permeation liquid membrane, PLM; diffusive gradients in thin films, DGT [12]). Finally, it is possible to physically separate dissolved Ag (Ag^+ and its complexes) from nAg using ultracentrifugation, ultrafiltration or centrifugal ultrafiltration [11,12,15,16]. Each of the methods has its own advantages and limitations, based upon implementation, cost, detection limits and whether or not free ions can be measured independently from the labile metal complexes.

In this study, three analytical techniques (IET; centrifugal ultrafiltration; single particle inductively coupled plasma mass spectrometry, SP ICP-MS) were evaluated for their ability to

---

* Corresponding author. Tel.: +1 514 343 6741; fax: +1 514 343 7586.
E-mail address: kj.wilkinson@umontreal.ca (K.J. Wilkinson).

0039-9140/$ - see front matter © 2012 Elsevier B.V. All rights reserved.
http://dx.doi.org/10.1016/j.talanta.2012.11.048

quantify free or dissolved Ag in suspensions of nAg. Particle dissolution was quantified for a wide range of nAg concentrations and under variable physicochemical conditions.

2. Materials and methods

2.1. Reagents

Dowex 50W-X8 (50–100 mesh, exchange capacity of 5.1 ± 1 meq/g, Sigma) was used as the cation exchange resin for the IET. Sodium hydroxide ($\geq 98\%$, 0.1 M) was used to convert the resin to its Na^+ form prior to use and sodium nitrate (99%, Sigma) was used as the swamping electrolyte. High purity nitric acid (65%, TraceSelectUltra) was purchased from Fluka. In some experiments, 2-[*N*-morpholino]-ethanesulfonate sodium salt (NaMES, Sigma-Aldrich) was used to buffer solutions to pH 6. Silver standards were prepared from a reference solution of 1000 ppm Ag in 2% HNO_3 purchased from Fisher Scientific. Commercial suspensions of silver nanoparticles were purchased from Vive Crop Protection (formerly ViveNano, product no. AD0223SRFD) and Ted Pella (Product nos. 15705-20SC, 15707-20SC and 15710-20SC). The Vive Nano product was provided as a 1.5 g/L aqueous suspension of nAg (measured by gravimetry) stabilized by sodium polyacrylate (silver content of the dried sample = 31%). The product has been well characterized in previous work, with results by transmission electron microscopy and fluorescence correlation spectroscopy showing that $> 90\%$ of the nanoparticles were in the size range of 1–10 nm [17]. The products purchased from Ted Pella corresponded to aqueous (non-stabilized) suspensions of three different particle sizes (20, 40, and 80 nm). These samples are used as electron microscopy size standards. However, in aqueous solution; they do have a tendency to aggregate in the absence of a stabilizer such as citrate. Free ion concentrations in the concentrated nAg stock solutions were below 2%. In order to approach equilibrium conditions as much as possible, all samples analyzed in this study were first equilibrated for 3 days at room temperature in a pH buffered media.

2.2. Instrumentation

Total Ag concentrations in solution were determined using a Varian AA240Z Zeeman atomic absorption spectrometer or a PerkinElmer NexION 300 × ICP-MS. SP ICP-MS experiments were also carried out using the NexION 300 ×. pH measurements were made using a 744 Metrohm pH-meter. Nanoparticle Tracking Analysis (NTA; Nanosight LM10) was used to verify particle diameter variations of the nAg. Centrifugal ultrafiltration was performed in a Heraeus Multifuge 1 S-R centrifuge.

2.3. Ion-exchange technique (IET)

The ion-exchange approach is based upon the equilibration of the free ion with a small amount of cation exchange resin. The resin mass is small enough so that it will not cause any perceptible changes to the equilibrium distribution of chemical species in solution. Nonetheless, several conditions must be satisfied in order to measure equilibrium concentrations of free ion (M^{n+}) [18,19]. First, M^{n+} should be the only species exchanged with the resin counter-ions (Na^+). Second, at equilibrium, the total number of exchange sites should be much greater than those occupied by the adsorbed metal ion. Finally, the sample should contain counter-ions at a concentration that is not affected by the ion-exchange process. Equations describing the ion-exchange equilibria are given in the Supporting information.

Prior to use, fine particles of the resin were removed by sedimentation–decantation in MilliQ water ($R > 18\ M\Omega$ cm, organic carbon $< 2\ \mu g\ L^{-1}$) [18]. The resin was then washed with 1.5 M nitric acid, rinsed with MilliQ water and oven dried at 60 °C. For each ion exchange column, 10 milligrams of dry resin were suspended in MilliQ water and the slurry was carefully drawn into cut polypropylene tubes (inner diameter: 1.65 mm, length: 15 mm) where it was maintained with a small amount of glass wool. Four replicate columns were used for each experimental condition. In this study, optimized steps were as follows: resin wash with 20 mL of 1.5 M HNO_3, resin rinse with 20 mL of MilliQ water, conversion of the resin to its Na^+ form with 20 mL of 0.1 M NaOH, rinse with MilliQ water to neutral pH, pre-equilibration with 20 mL of a solution of similar pH and ionic strength as the sample to be analyzed, equilibration with the sample, rinse with MilliQ water (ca. 5 mL) and elution of adsorbed silver into pre-weighed polypropylene containers using 1.5 M HNO_3. At the end of each step, air was passed through the column to remove any remaining interstitial solution. Samples and wash solutions were pumped (Gilson Minipuls 3 peristaltic pump) through the resin columns at 5 mL/min while the elution was performed at 0.5 mL/min.

2.4. Single particle ICP-MS (SP ICP-MS)

SP ICP-MS was used for the simultaneous measurement of dissolved and nAg. The theoretical basis of SP ICP-MS has been described by Degueldre et al. [20–22] for natural metal colloids and by Laborda et al. [23] for the discrimination of ionic and nano silver. SP ICP-MS distinguishes between dissolved and particulate silver based upon their differing signal intensities in a highly diluted sample. Indeed, the sample must be sufficiently diluted so that, during the defined short detection interval (dwell time), only a single particle attains the mass spectrometer. Since dissolved metal is homogeneously distributed in the nebulized sample droplets, it will produce a constant signal, whereas the observation of additional, discrete signal pulses can be attributed to the ionization of nanoparticles (Fig. S1). The relative proportions of ions and nanoparticles are then determined from a statistical distribution of their pulse intensities. In this work, data acquisition parameters in the single particle mode were as follows: sweeps per reading: 1; readings per replicate: 20,000; dwell time: from 0.1 to 5 ms (3 ms dwell times were reported here, however, all studied dwell times led to similar conclusions); integration time 2.5 s.

2.5. Centrifugal ultrafiltration

The centrifugal filter units (Amicon ultra, 3 kDa molar mass cutoff) were first pre-equilibrated with the sample matrix (free of Ag, same *I* and pH). Subsequently, 4 mL of each sample were centrifuged at $3700 \times g$ for 20 min over four centrifugation cycles in order to equilibrate the filters with the Ag (Fig. S2), which reduces adsorptive losses of Ag^+. At the end of each centrifugation cycle, all liquid was removed from the devices. Following the final cycle, dissolved silver concentrations were determined in the filtrate while nAg was determined from an analysis of the silver remaining in the retentate. Samples indicating a deviation of greater than 10% from the theoretical mass balance were rejected.

3. Results and discussion

3.1. Optimization of the IET for determinations of Ag^+

For measurements of Ag^+ to be valid, the resin must be at equilibrium with the sample. Equilibrium is verified by percolating the samples through the column until [Ag] in the sample = [Ag] in the effluent (Fig. 1). Equilibration was assured by employing sufficiently large sample volumes, corresponding to relatively long

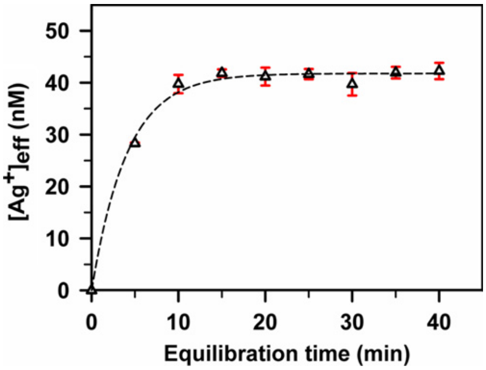

Fig. 1. Variation of silver in the effluent as a function of contact time for a column containing 10 mg of a Dowex 50W-X8 resin. The concentration of Ag^+ in the inflow was 41.7 nM; flow rate=5 mL/min, pH=6, $[NaNO_3]=0.05$ M.

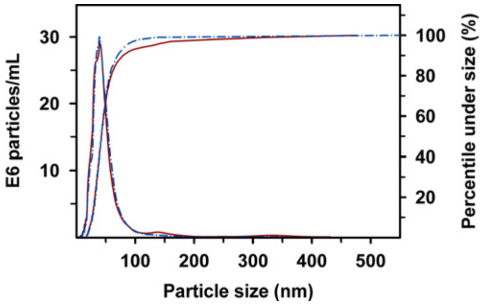

Fig. 2. NTA particle size measurements of non-coated nAg (Ted Pella, 40 nm) before (continuous line) and after (dash-dotted line) percolation through a mini-column containing 50 mg of cation exchange resin (Dowex 50W-X8); nominal particle size: 40 nm, total silver concentration: 3.7 μM.

equilibration times. Due to the interaction of H^+ with the resin, the pH must be carefully controlled or the standards prepared precisely at the same pH as the samples. With this resin, pH 4 is likely the lower limit at which one can operate the IET due to proton competition [24]. For a medium buffered to pH 6 with 10^{-3} M MES (2-[*N*-morpholino]-ethanesulfonate) at an ionic strength of 0.05 M, the mean distribution coefficient (metal bound to resin divided by that in solution) obtained from triplicate measurements was 1.20 ± 0.05 L/g. Under these conditions, detection limits calculated from the standard deviation ($n=5$) of the 68 nM sample gave 2.5 nM. The precision and accuracy of the IET were verified using standard solutions of silver ions and mixtures of ions and nanoparticles. For example, strongly linear relationship ($R^2=0.98$) was determined between the resin bound silver (determined after elution) and Ag^+ concentrations in solution (Fig. S3). Furthermore, repeated measurements of the distribution coefficient were constant ($\pm <5\%$) under the experimental conditions mentioned above.

In order to confirm that nAg particles were not retained by the resin, the coated and non-coated nanosilver suspensions were percolated through the IET columns and fractions were collected at different times (1–20 min) for analysis by NTA. NTA measurements showed no variation in particle size or particle concentration before and after passing through the resin (Fig. 2). In addition, the breakthrough curve for the nAg suspension was very similar to that observed for the silver ions (Fig. S4). The small amount of silver retained in the first volume fraction was due to the presence of silver ions in the nAg suspension.

The IET was used to measure free Ag^+ in several concentrations of (coated and non-coated) nanosilver suspensions. For samples prepared by dilution of a given stock solution, free Ag increased with increasing particle concentration (Fig. 3, solid points), as would be expected. Somewhat counter-intuitively, proportionally more Ag^+ was observed for the higher dilutions (lower particle concentrations).

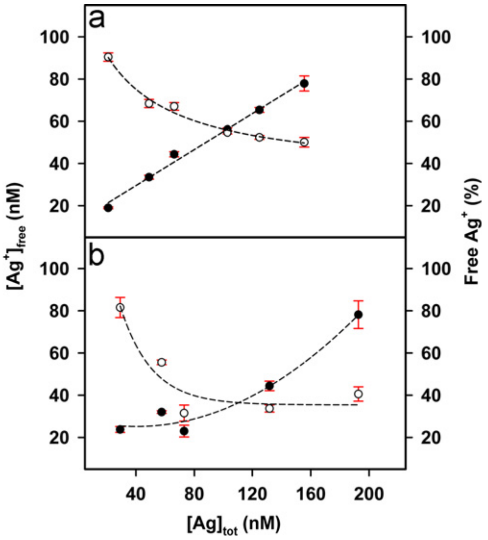

Fig. 3. Evolution of free Ag^+ for different dilutions of nAg obtained using the IET technique: (a) PAA stabilized nAg (Vive Nano); (b) non-coated nAg (Ted Pella, 20 nm). The concentration of dissolved silver is given in nanomolar (nM) (●) while its proportion with respect to nAg is given as % (○); $I=0.05$ M $NaNO_3$, pH=6. Samples were equilibrated for 72 h before measurement.

3.2. *Centrifugal ultrafiltration and SP ICP-MS*

Given that it was somewhat unexpected to find proportionally more particle dissolution/oxidation at lower particle concentrations, two complementary techniques were employed to verify dissolved Ag concentrations: centrifugal ultrafiltration (Fig. 4) and SP ICP-MS (Figs. 5 and 6). Due to the different detection limits, examined concentrations were not precisely the same for all of the techniques (compare *x*-axes of Figs. 3–6). Furthermore, for the smallest nAg (below 20 nm), nAg was not observed using SP ICP-MS and thus only data for the 80 nm nAg are given in Figs. 5 and 6. Results were globally consistent using all three techniques, for both particle types and all particle sizes, i.e. higher nAg concentrations resulted in higher free or dissolved Ag and proportionally higher dissolution was observed at the lower particle concentrations.

As observed using the other techniques, the results obtained by SP ICP-MS demonstrated a clear decrease in the proportion of free Ag^+ with an increasing concentration of nAg. This point is clearly shown in Fig. S5, where results from all three analytical techniques have been compiled in a single figure. Furthermore, the SP ICP-MS intensity histograms clearly showed a decreasing nAg signal as the suspension was diluted. For example, the average peak intensity corresponding to the nAg decreased from 13159 to 1704 counts (8 fold decrease) as the suspension was diluted from 12.9 nM to 2.6 nM (5 fold decrease) resulting in a proportionally larger decrease in the nAg contribution (Fig. 5). In parallel, the signal corresponding to dissolved silver leveled off at the higher total Ag concentrations, resulting in a significantly smaller contribution of the nanoparticles to the total as the suspensions are diluted (Fig. 6), reinforcing the hypothesis of dissolution at low concentrations.

Four plausible mechanisms could explain the increased particle dissolution at the lower particle concentrations, namely, increased Ag^+ release due to (i) particle oxidation ($Ag^0 \rightarrow Ag^+$); (ii) increased Ag^+ desorption from the particle surfaces (including the carboxyl groups of the coatings, $Ag\text{-}X \rightarrow Ag^+ + X$); (iii) increased *dissolution*

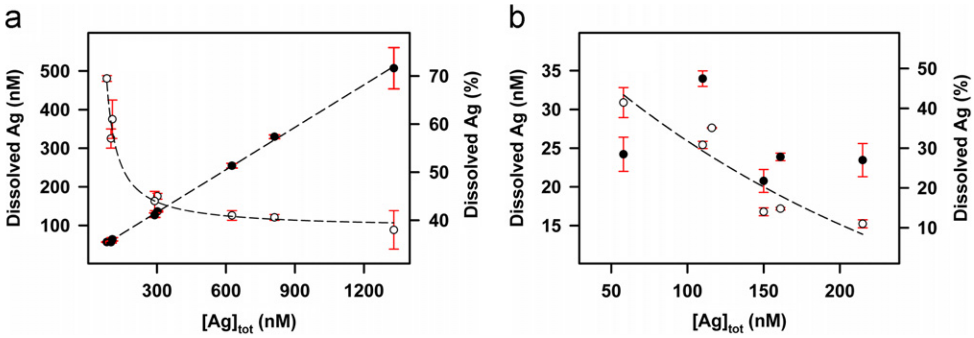

Fig. 4. Evolution of dissolved Ag for different dilutions of total silver obtained using centrifugal ultrafiltration: (a) PAA stabilized nAg (Vive Nano); (b) non-coated nAg (Ted Pella, 20 nm). The concentration of dissolved silver is given in nM (●) while its proportion with respect to nAg is given by the open points % (○); I=0.05 M $NaNO_3$, pH=6. Samples were equilibrated for 72 h before measurement.

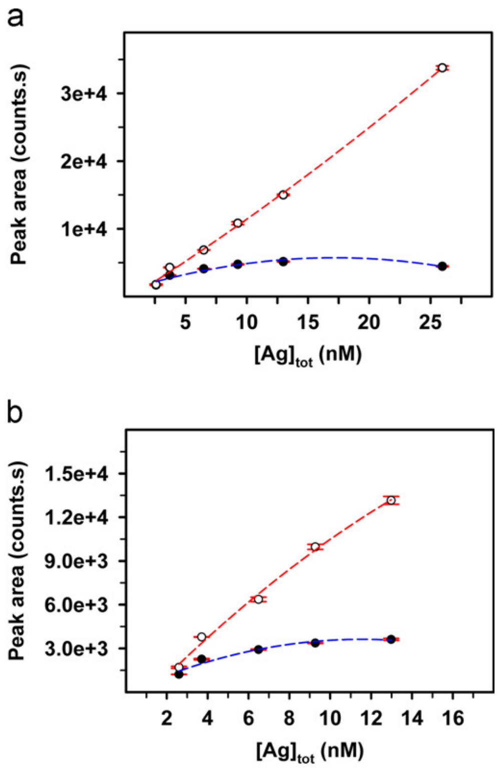

Fig. 5. SP ICP-MS measurements of (○) nAg and (●) dissolved Ag in (a) a freshly prepared and (b) equilibrated (3d) suspension of silver nanoparticles (Ted Pella, 80 nm). Variations of the measured areas are presented as a function of total Ag concentration.

of poorly soluble species ($Ag_2L \rightarrow 2\ Ag^+ + L^{2-}$) or (iv) increased Ag *complexation* in solution ($Ag^+ + Y^- \rightarrow AgY$).

While the presence of a constant concentration of a silver binding ligand in solution could result in a larger proportion of dissolved Ag at higher dilutions (due to decreasing metal: ligand ratio), this is unlikely to have occurred here. The use of simple electrolyte solutions containing only $NaNO_3$ suggests that neither Ag precipitates nor Ag complexes were likely to form. Furthermore, while the centrifugal ultrafiltration and the SP ICP-MS measure dissolved (Ag^+ and its complexes) as opposed to free Ag, the dilution effect was also observed using IET measurements, which only measures Ag^+. While many silver halides, including AgCl, are poorly soluble in water, these species were carefully avoided here. In addition, neither Ag_2O nor Ag_2CO_3 were predicted to occur from thermodynamic considerations ($pK_{sp}(Ag_2O)=10.44$; $pK_{sp}(Ag_2CO_3)=11.09$). The absence of added ligands and the observed undersaturation of Ag species strongly suggests that neither complexation (iv) nor precipitation (iii) were responsible for the observation of proportionally increasing Ag^+.

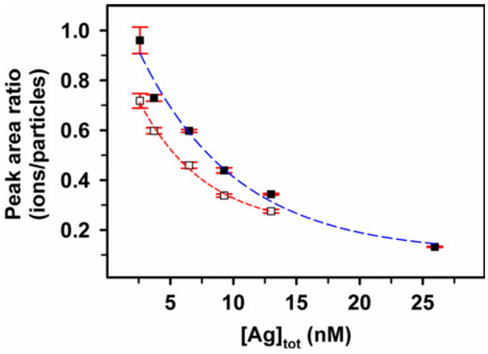

Fig.6. SP ICP-MS determinations of the proportion of dissolved silver and nAg particles in freshly prepared (■) and 3 day equilibrated (□) suspensions of nAg (Ted Pella, 80 nm). Variation of the ratio of peak areas (dissolved/nanoparticles) as a function of the total metal concentration.

The remaining explanations, i.e. increased surface desorption or increased oxidation at low nAg concentrations, would appear to be consistent with all of the experimental observations. In the case of surface adsorbed Ag^+, sample dilution should indeed drive the equilibrium toward greater Ag^+ in solution. Nonetheless, since nAg includes both the core nAg and the adsorbed species, the effect should be more obvious for smaller nAg, where surface atoms are a smaller proportion of particle mass, which was not the case here, i.e. no differences in $[Ag^+]/[nAg]$ were identified for the different particle sizes. On the other hand, depletion of either protons or O_2 could potentially limit Ag^+ production, especially for the higher concentrations of nAg. Indeed, thermodynamic calculations [11] and the above results suggest that nAg will not persist in environmentally relevant, oxic waters. The rate of Ag^0 oxidation is increased by the presence of oxygen, low pH and low particle concentrations, while it is decreased by the presence of natural organic matter (NOM) [11]. While Liu and Hurt [11] produced an empirical relationship to predict nAg dissolution, we would argue that due to the abundance of factors affecting both the kinetics and thermodynamics of the oxidation reaction in natural systems (nature of the nAg, presence of a stabilizer such as NOM, temperature, oxygen, pH, etc.), it will always be necessary to carefully measure Ag^+ concentrations in order to rigorously distinguish between the effects of Ag^+ and nAg. Given that the partitioning of Ag^+/nAg depends upon the precise physicochemical conditions of the medium, including particle concentration; risk assessments of nAg will need to be performed concurrently with analytical measurements of dissolution made under identical conditions (especially concentration and equilibration time).

4. Conclusions

Three techniques for determining dissolved [Ag] (SP ICP-MS; centrifugal ultrafiltration) or Ag^+ (IET) were evaluated here. Centrifugal ultrafiltration is surely the most straightforward of the techniques; however, it typically gave the highest variability and detection limits. In order to reduce the adsorption of dissolved metal to the ultrafiltration membrane at the lowest concentrations, it was necessary to pre-equilibrate the membranes with a large excess of experimental solution. SP ICP-MS provided the most information (including particle sizes). However, the dynamic range of the technique was limited to a very narrow range of (low) particle concentrations. It was nonetheless the most rapid technique, requiring the smallest sample volumes (less than 1 mL). The use of the ion exchange resin provided high sensitivity (samples were concentrated on the resins) at low cost, with arguably the most environmental relevance (measurement of Ag^+ rather than dissolved Ag). Furthermore, it was appropriate for analyzing a wide range of free metal concentrations (2.5×10^{-9} M–1.0×10^{-7} M in this study). This concentration range can be extended depending upon the mass of resin used, the ionic strength and pH. On the other hand, the IET required large sample volumes (ca. 200 mL), relative to SP ICP-MS and centrifugal ultrafiltration and significant sample processing time. In any case, toxicological and environment insight will be greatly improved through the use of any or a combination of these techniques.

Acknowledgments

Funding for this work was provided by the Natural Sciences and Engineering Research Council of Canada (NRC-NSERC-BDC nanotechnology initiative and NSERC strategic grant). Some of the nAg particles used in this study were donated by Vive Nano.

Appendix A. Supporting information

Supplementary data associated with this article can be found in the online version at http://dx.doi.org/10.1016/j.talanta.2012.11.048.

References

[1] N. Lubick, Environ. Sci. Technol. 42 (2008) 8617 8617.
[2] H.J. Johnston, G. Hutchison, F.M. Christensen, S. Peters, S. Hankin, V. Stone, Crit. Rev. Toxicol. 40 (2010) 328–346.
[3] M. Ahamed, M.S. AlSalhi, M.K.J. Siddiqui, Clin. Chim. Acta. 411 (2010) 1841–1848.
[4] P.D. Bragg, D.J. Rainnie, Can. J. Microbiol 20 (1974) 883–889.
[5] E.I. Tserovsky, S. Arpadjan, D.L. Tsalev, Spectrosc. Lett. 25 (1992) 693–705.
[6] J.S. Kim, E. Kuk, K.N. Yu, J.H. Kim, S.J. Park, H.J. Lee, S.H. Kim, Y.K. Park, Y.H. Park, C.Y. Hwang, Y.K. Kim, Y.S. Lee, D.H. Jeong, M.H. Cho, Nanomed. Nanotechnol. 3 (2007) 95–101.
[7] S. Kheybari, N. Samadi, S.V. Hosseini, A. Fazeli, M.R. Fazeli, Daru J. Pharm. Sci. 18 (2010) 168–172.
[8] P.V. Asharani, Y. Lian Wu, Z. Gong, S. Valiyaveettil, Nanotechnology 19 (2008) 255102, DOI 255110.251088/250957-254484/255119/255125/255102..
[9] R. Foldbjerg, P. Olesen, M. Hougaard, D.A. Dang, H.J. Hoffmann, H. Autrup, Toxicol. Lett. 190 (2009) 156–162.
[10] N. Miura, Y. Shinohara, Biochem. Biophys. Res. Commun. 390 (2009) 733–737.
[11] J.Y. Liu, R.H. Hurt, Environ. Sci. Technol. 44 (2010) 2169–2175.
[12] E. Navarro, F. Piccapietra, B. Wagner, F. Marconi, R. Kaegi, N. Odzak, L. Sigg, R. Behra, Environ. Sci. Technol. 42 (2008) 8959–8964.
[13] M. Pesavento, G. Alberti, R. Biesuz, Anal. Chim. Actas 631 (2009) 129–141.
[14] T.M. Benn, P. Westerhoff, Environ. Sci. Technol. 42 (2008) 4133–4139.
[15] R.F. Domingos, D.F. Simon, C. Hauser, K.J. Wilkinson, Environ. Sci. Technol. 45 (2011) 7664–7669.
[16] J. Fabrega, S.R. Fawcett, J.C. Renshaw, J.R. Lead, Environ. Sci. Technol. 43 (2009) 7285–7290.
[17] T.O. Peulen, K.J. Wilkinson, Environ. Sci. Technol. 45 (2011) 3367–3373.
[18] F.F. Cantwell, J.S. Nielsen, S.E. Hrudey, Anal. Chem. 54 (1982) 1498–1503.
[19] I.A.M. Worms, K.J. Wilkinson, Anal. Chim. Acta 616 (2008) 95–102.
[20] C. Degueldre, P.Y. Favarger, Colloid Surf. A 217 (2003) 137–142.
[21] C. Degueldre, P.Y. Favarger, S. Wold, Anal. Chim. Acta 555 (2006) 263–268.
[22] C. Degueldre, P.Y. Favarger, R. Rosse, S. Wold, Talanta 68 (2006) 623–628.
[23] F. Laborda, J. Jimenez-Lamana, E. Bolea, J.R. Castillo, J. Anal. Atom. Spectrom. 26 (2011) 1362–1371.
[24] T. Sato, J. Radioanal. Nucl. (1978) 81–91 Chapter 43.